NUMERICAL INVESTIGATION OF COMBUSTION BEHAVIOR INDUCED BY SHOCK WAVE IN COMBUSTIBLE JET TRAINS

Miyashita M.[1], Matsuo A.[2], Shima E.[3], Itouyama N.[4], Kawasaki A.[5], Matsuoka K.[6], Kasahara J.[7]
[1] Graduate School of Science and Technology, Keio University, 3-14-1 Hiyoshi, Kohoku-ku, Yokohama, Kanagawa, 223-8522, Japan, moenomiyashit@keio.jp
[2] Department of Mechanical Engineering, Keio University, 3-14-1 Hiyoshi, Kohoku-ku, Yokohama, Kanagawa, 223-8522, Japan, matsuo@mech.keio.ac.jp
[3] Department of Mechanical Engineering, Keio University, 3-14-1 Hiyoshi, Kohoku-ku, Yokohama, Kanagawa, 223-8522, Japan, shima.eiji@jaxa.jp
[4]Department of Aerospace Engineering, Nagoya University, Furo-cho, Chikusa-ku, Nagoya, Aichi, 464-8603, Japan, itouyama@imass.nagoya-u.ac.jp
[5]Department of Mechanical Engineering, Shizuoka University, 3-5-1, Jyohoku, Naka-ku, Hamamatsu, Shizuoka, 432-8561, Japan, kawasaki.akira@shizuoka.ac.jp
[6]Department of Aerospace Engineering, Nagoya University, Furo-cho, Chikusa-ku, Nagoya, Aichi, 464-8603, Japan, matsuoka@nuae.nagoya-u.ac.jp
[7]Department of Aerospace Engineering, Nagoya University, Furo-cho, Chikusa-ku, Nagoya, Aichi, 464-8603, Japan, kasahara@nuae.nagoya-u.ac.jp

ABSTRACT

Hydrogen-fueled engines have been actively developed to realize a carbon-neutral society. On the other hand, in developing these engines, it is necessary to prevent unexpected explosions and detonation wave propagation with hydrogen leakage from the hydrogen storage system or engine piping. This study conducted two-dimensional numerical analyses for the detonation propagating in combustible H_2-O_2 jet trains to clarify the combustion behavior in the hydrogen leaking area. An H_2-O_2 premixed or non-premixed gas flowed from the bottom at a fixed mass flow rate to reproduce the fuel leakage. A 100 mm long and 100 mm high leakage area was used to simulate an open area outside the combustor or pipeline. The detonation was entered from the pre-detonator, installed at the lower left of the leakage area. As a result, the detonation, which entered at 2702 m/s, sustained propagation in the premixed jet train leaking area. In the case with the largest amount of leakage, the propagation velocity decreased to 1910 m/s immediately after the entry into the leakage area and remained close to the C-J velocity. On the other hand, in the non-premixed jet train with three different equivalence ratios, the detonation propagation was not maintained in the non-premixed inflow condition, even though the propagation was maintained in the premixed inflow condition.

1.0 INTRODUCTION

In recent years, using renewable energy to replace hydrocarbon-based fuels has been promoted to realize a carbon-neutral society. For example, in the air transportation field, aircraft engines that use renewable energy are actively developing in response to ICAO (International Civil Aviation Organization)'s policy which has no increase in greenhouse gas emissions in 2050 compared to 2019 [1]. One of the typical renewable energy sources is hydrogen. Compared to other renewable energy sources, hydrogen does not emit NOx or SOx during combustion and is not expensive to produce. Therefore, developing hydrogen-fueled combustors and safety management technologies has been pursued, especially in Europe [1].

To use hydrogen as a fuel, it needs to be safe as conventional hydrocarbon-based fuels. The flammable range of hydrogen is much more comprehensive than that of conventional fuels such as CH_4 and C_3H_8, and the minimum ignition energy is the order of 10^{-2} mJ, much smaller than conventional fuel [2]. An unexpected leak or ignition from the hydrogen storage system or engine piping is expected to result in an explosion that causes more extensive damage than conventional fuels. In particular, the most

extensive damage from an unexpected explosion occurs when a detonation wave propagates. Detonation is a combustion wave propagating at 5-10 times the speed of sound accompanied by a shock wave. It comprises a leading shock wave, an induction zone, and a reaction zone. Since its discovery at the end of the 19th century [3], detonation has been treated as a combustion phenomenon that causes the most extensive damage in an explosion. Preventing the occurrence of detonation has been considered an essential factor in assuring safety.

Many experimental and numerical studies have been conducted on detonation's occurrence and propagation persistence. For example, Burr et al. [4] conducted an experimental study about the wavefront structure of a detonation as it enters a combustible jet stream with hydrocarbon fuels. Faming et al. [5] also conducted numerical and experimental studies on the propagation velocity of detonations on combustible jet trains. However, these studies were only analyses of detonation behavior which propagates continuously, and knowledge on the onset of detonation simulating fuel leakage is still needed. For these backgrounds, it is necessary to investigate the most dangerous conditions under which detonation propagates when fuel leaks.

This study investigates the relationship between the propagation persistence of detonation and the state of hydrogen leakage from the engine piping or the combustor to the open area. In particular, the following three conditions were assumed and analyzed by gradually simulating leakage conditions that are close to reality, starting from the most modeled leakage condition：

1. Detonation enters H_2-O_2 premixed gas quiescently distributed in the open area.

2. Detonation enters H_2-O_2 premixed gas leaking from the multiple leakage ports. Three cases were set and compared concerning different amounts of leakage relative to the area.

3. Detonation enters in H_2-O_2 non-premixed gas leaking from the multiple leakage ports. Three cases were set and compared concerning different equivalent ratio.

2.0 NUMERICAL METHODS

In this study, the two-dimensional compressible Navier-Stokes equation and the conservation laws for nine chemical species (H_2, O_2, H, O, OH, H_2O, HO_2, H_2O_2, and N_2) shown below were used as the governing equations for the numerical analyses. To enclose this system, the equation of state was used, assuming thermally perfect gases condition.

$$\frac{\partial \hat{\mathbf{Q}}}{\partial t}+\frac{\partial(\hat{\mathbf{E}}-\hat{\mathbf{E}}_{\mathbf{v}})}{\partial \xi}+\frac{\partial(\hat{\mathbf{F}}-\hat{\mathbf{F}}_{\mathbf{v}})}{\partial \eta}=\hat{\mathbf{S}} \tag{1}$$

$$\hat{\mathbf{Q}}=\frac{1}{J}\begin{bmatrix}\rho\\ \rho u\\ \rho v\\ e\\ \rho_i\end{bmatrix},\ \hat{\mathbf{E}}=\frac{1}{J}\begin{bmatrix}\rho U\\ \rho uU+\xi_x p\\ \rho vU+\xi_y p\\ (e+p)U\\ \rho_i U\end{bmatrix},\hat{\mathbf{E}}_{\mathbf{v}}=\frac{1}{J}\begin{bmatrix}0\\ \xi_x\tau_{xx}+\xi_y\tau_{xy}\\ \xi_x\tau_{yx}+\xi_y\tau_{yy}\\ \xi_x\beta_x+\xi_y\beta_y\\ \xi_x\rho D_i\dfrac{\partial Y_i}{\partial x}+\xi_y\rho D_i\dfrac{\partial Y_i}{\partial y}\end{bmatrix},$$

$$\hat{\mathbf{F}}=\frac{1}{J}\begin{bmatrix}\rho V\\ \rho uV+\eta_x p\\ \rho vV+\eta_y p\\ (e+p)V\\ \rho_i V\end{bmatrix},\hat{\mathbf{F}}_{\mathbf{v}}=\frac{1}{J}\begin{bmatrix}0\\ \eta_x\tau_{xx}+\eta_y\tau_{xy}\\ \eta_x\tau_{yx}+\eta_y\tau_{yy}\\ \eta_x\beta_x+\eta_y\beta_y\\ \eta_x\rho D_i\dfrac{\partial Y_i}{\partial x}+\eta_y\rho D_i\dfrac{\partial Y_i}{\partial y}\end{bmatrix},\hat{\mathbf{S}}=\frac{1}{J}\begin{bmatrix}0\\ 0\\ 0\\ 0\\ \omega_i\end{bmatrix} \tag{2}$$

$$e = \sum_i \rho_i h_i - p + \frac{1}{2}\rho(u^2 + v^2) \tag{3}$$

$$\beta_x = \tau_{xx}u + \tau_{xy}v + \kappa\frac{\partial T}{\partial x} + \rho\sum_i^N h_i D_i \frac{\partial Y_i}{\partial x} \tag{4}$$

$$\beta_y = \tau_{yx}u + \tau_{yy}v + \kappa\frac{\partial T}{\partial y} + \rho\sum_i^N h_i D_i \frac{\partial Y_i}{\partial y} \tag{5}$$

$$p = \sum_i^N \rho_i R_i T \tag{6}$$

where ρ – density; u - x direction velocity ; v - y direction velocity ; p – pressure ; e - total energy ; T – temperature ; J – Jacobian ; τ - shear stress ; μ – viscosity ; κ - thermal conductivity ; D - diffusion coefficient ; Y - mass fraction ; ω - reaction rate ; h – enthalpy ; R - gas constant ; N - the number of chemical species ; subscript i means the ith species.

The convection term was discretized by AUSMDV [6], the third ordered by MUSCL method, and three steps third ordered TVD Runge-Kutta method [7] was used for the time integration of the fluid. The chemical reaction model proposed by Hong et al. [8] was used, which considered 20 elementary reactions of 9 chemical species, and the point-implicit method was used as the time integration method for the source term.

3.0 COMPUTATIONAL DOMAIN

Figure 1 shows the computational target used in the analyses. In this study, a leakage area was used to simulate an open area. A pre-detonator was installed in the lower left corner of the leakage area to simulate an unexpected detonation.

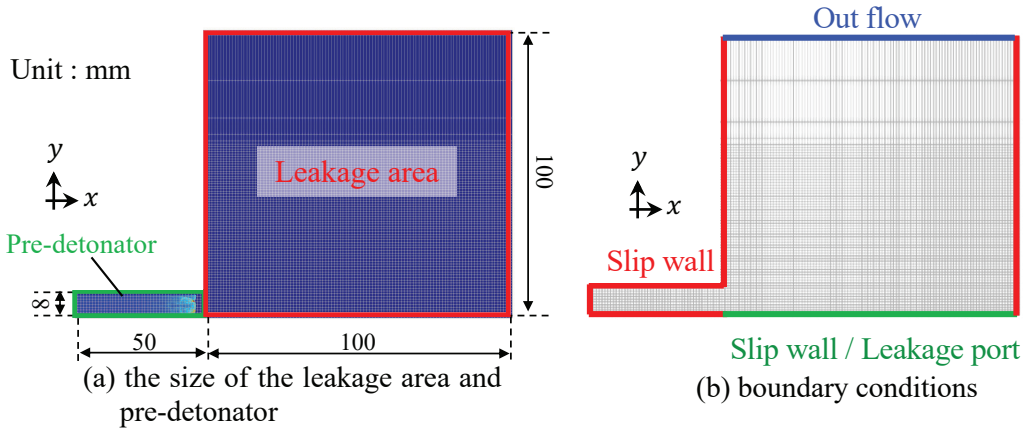

Figure 1. Details of computational domain and calculation grids (every 25 points)

3.1 Pre-detonator

Figure 2 shows the well-developed detonation propagated in the pre-detonator. The height of the pre-detonator was 8 mm, and the length was 50 mm. $2H_2$-O_2 premixed gas was uniformly distributed, where the total pressure and temperature were set to 15 kPa and 295 K. The induction length and C-J velocity in this unburned mixture condition were 389.6 μm and 2733 m/s. The boundary condition was set as slip walls because the effect of the wall surface on the flow field was ignored, as shown in Fig. 1(b). The grid size was 20 μm and the number of grid points was 1.0×10^6 pts. Figure 2 shows (a) the instantaneous pressure field, (b) the temperature field, and (c) the maximum pressure history in the pre-detonator with the detonation propagating under the above condition. A well-developed detonation propagated at 2702 m/s, which was 98.9% of the C-J velocity, and whose cell size was 3.88±0.42 mm.

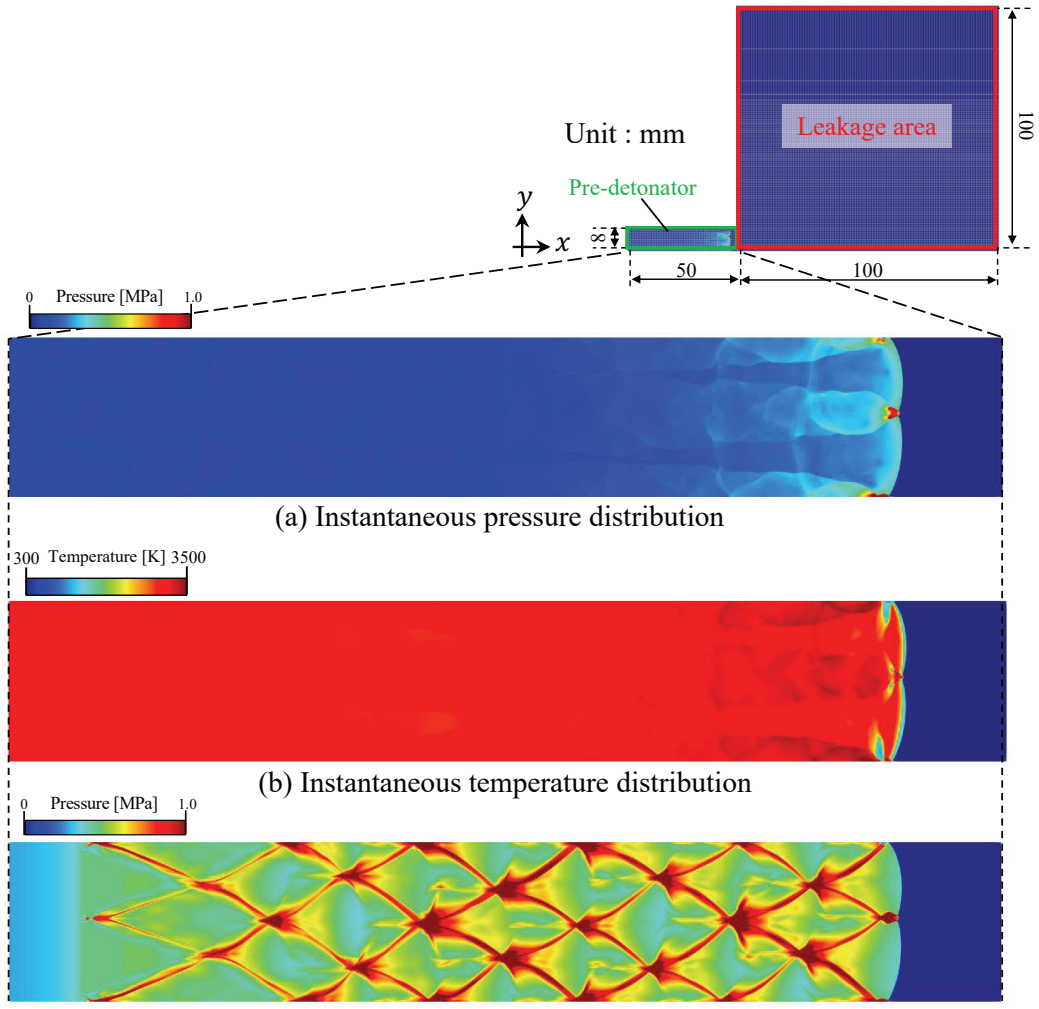

Figure 2. Fully developed detonation propagated in the pre-detonator

3.2 Initial conditions of leakage area

The leakage area used in the analysis is shown in Fig. 1 (a), and boundary conditions are given as shown in Fig. 1 (b). The height and length of the area was 100 mm which was wide enough to analyze the entering detonation to leakage area. The minimum grid size was 20 μm and the number of grid points was 22.5×10^6 pts.

In this study, three leaked conditions were set as the initial condition of the leakage area to gradually simulate leakage conditions that are close to reality, starting from the most modeled leakage condition. Firstly, H_2-O_2 stoichiometric premixed gas, where the total pressure and temperature were set to 15 kPa and 295 K, was uniformly distributed in the leakage area to simulate the uniform leakage outside the combustor, as shown in Fig. 3.

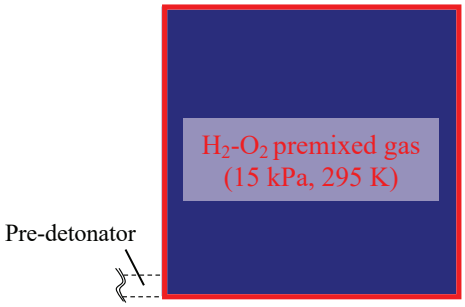

Figure 3. Initial condition of uniformly distributed premixed H_2-O_2

Second, H_2-O_2 stoichiometric premixed gas, where the total pressure and temperature were set to 15 kPa and 295 K flowed in from the bottom of the leakage area. Three kinds of leakage conditions, case p-3.75, case p-7.5, and case p-11.5, were set to examine the difference in the amount of leakage. Figure 4 shows the three leaked conditions and inflow boundary conditions. Multiple leakage points were placed at the bottom of the leakage area, each spaced at 3.75 mm, 7.5 mm, and 11.5 mm, and premixed gas continuously flowed into the channel for 20 μs. The total height of the leaked fuel was approximately 18 mm in all three cases, and the averaged atmospheric pressure, temperature, and the area of fuel distribution in the leakage area are shown in Table 1.

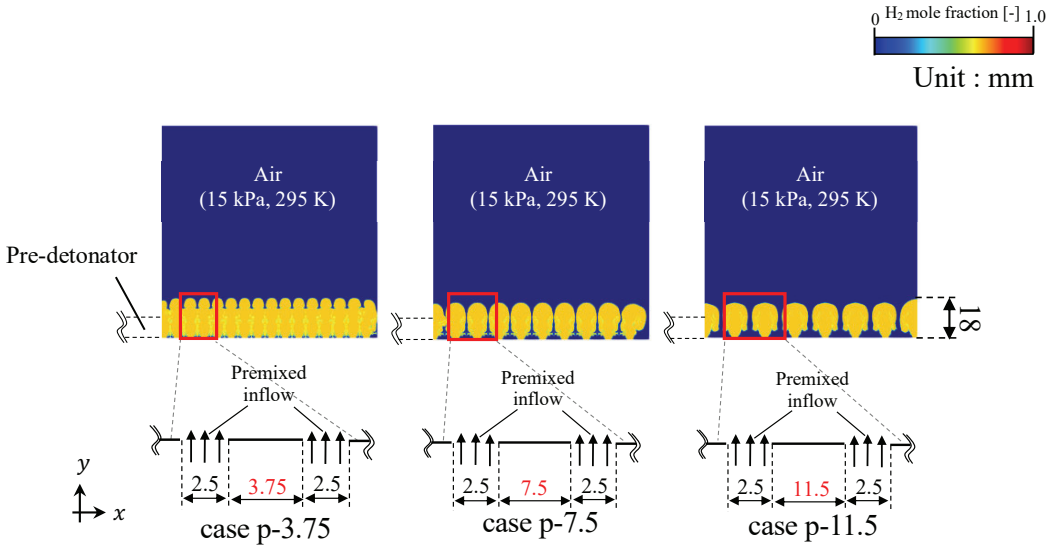

Figure 4. Inflow conditions of case p-3.75, case p-7.5, and case p-11.5, which premixed gas leaked from the multiple leakage ports

Table 1. Averaged pressure, temperature and fuel distribution area of case p-3.75, case p-7.5, and case p-11.5

	averaged pressure [MPa]	averaged temperature [K]	fuel distribution area [mm^2]
case p-3.75	0.039	229	1704
case p-7.5	0.029	240	1369
case p-11.5	0.025	251	1186
initial condition before leaking	0.015	295	0

Thirdly, H_2-O_2 non-premixed gas, where the total pressure and temperature were set to 15 kPa and 295 K, flowed in from the bottom of the leakage area. In this leaked condition, the following three cases were set: case n-3.75_3.0, case n-3.75_1.0, and case n-3.75_0.4, and compared concerning different equivalence ratios of the mixture condition by changing the width of H_2 leakage ports. Figure 5 shows the three leaked conditions and inflow boundary conditions. At the bottom of the leakage area, 16 leakage points were placed spaced with 3.75 mm intervals, which equivalence ratios were 3.0, 1.0, and 0.4, continuously flowing into the leakage area for 20 μs. The fill height of the leaked hydrogen was about 11 mm in the three cases, and the averaged atmospheric pressure, temperature, and area of fuel distribution in the leakage area are shown in Table 2.

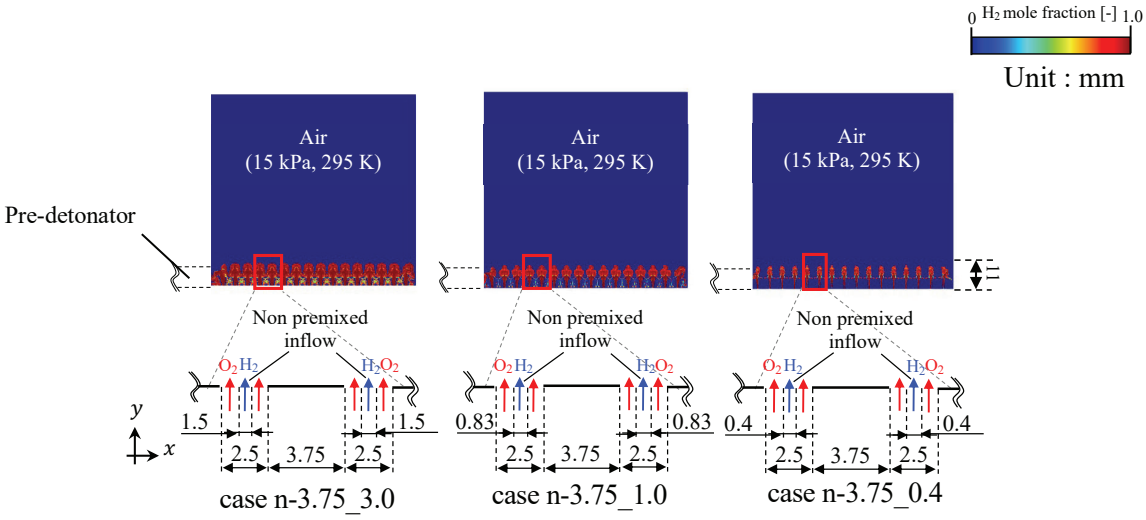

Figure 5. Inflow conditions of case n-3.75_3.0, case n-3.75_1.0, and case n-3.75_0.4, which non-premixed gas leaked from the multiple leakage ports

Table 2. Averaged pressure, temperature and fuel distribution area of case n-3.75_3.0, case n-3.75_1.0, and case n-3.75_0.4

	averaged pressure [MPa]	averaged temperature [K]	fuel distribution area [mm^2]
case n-3.75_3.0	0.039	229	668
case n-3.75_1.0	0.043	281	609
case n-3.75_0.4	0.037	288	668

4.0 RESULTS AND DISCUSSION

4.1 Behavior in uniformly distributed premixed H_2-O_2

Figure 6 shows the instantaneous pressure and temperature fields after the detonation entered the uniformly distributed premixed gas. The fully developed detonation propagated through the pre-detonator and entered from the left in the figure, and the shock wave propagated in the leakage area. In Fig. 6, for the pressure field, the shock wave propagated from the bottom left to the top right and gradually weakened as it propagated. It suggests that sufficient pressure buildup by combustion has not been achieved. In addition, shock and flame front decoupling was observed in the temperature field, and detonation did not sustain propagation.

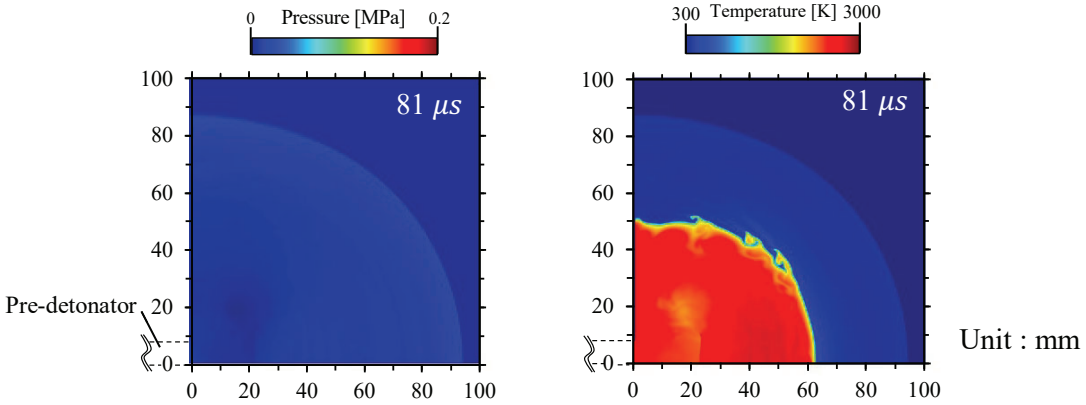

Figure 6. Instantaneous pressure and temperature fields

4.2 Behavior in premixed H_2-O_2 leakage

Figures 7 and 8 show instantaneous pressure and temperature fields under the premixed leakage condition, 29 μs, 80 μs, and 81 μs for each case after the detonation entered in leakage area. The detonation propagated through the pre-detonator and entered in leakage area, and the shock wave propagated in the leakage area. In the three cases with leakage from the bottom, the shock wave and the reaction zone were coupled immediately behind, and detonation maintained propagation. The greater the leakage and uniform distribution of premixed gas, the stronger the pressure rise at the wavefront. In particular, case p-3.75, with the largest leakage, had the strongest developed detonation compared to the other cases.

The shock wave position and the time evolution of the propagation velocity are shown in Fig. 9 and 10 for the three cases in which detonation propagation was confirmed. In Fig.9, the propagation velocities in cases p-11.5 and p-7.5 showed similar trends, and the propagation velocity reached a constant value with time evolution. On the other hand, in case p-3.75, the propagation velocity decreased to 1910 m/s immediately after the entry into the leakage area and accelerated to about 2500 m/s, which is comparable to the C-J velocity. This means that the propagation of well-developed detonation was maintained only in case p-3.75.

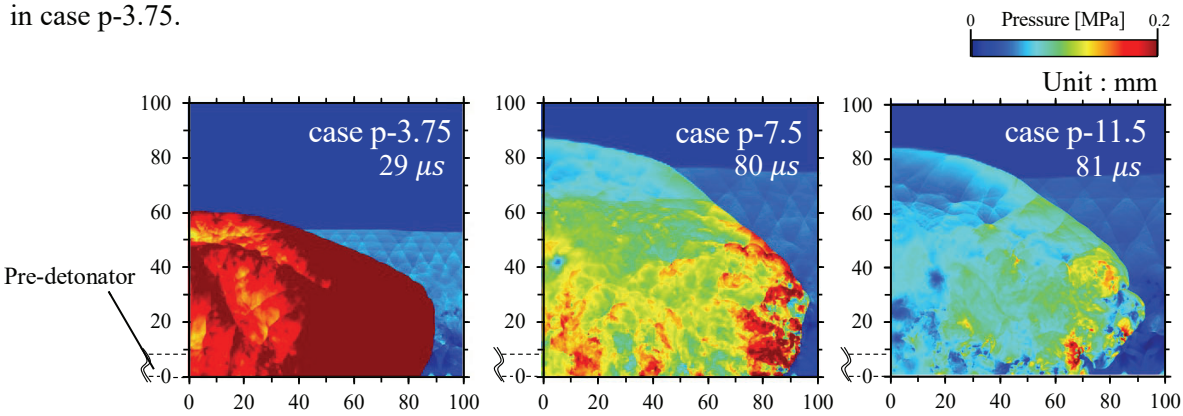

Figure 7. Instantaneous pressure fields of each premixed case

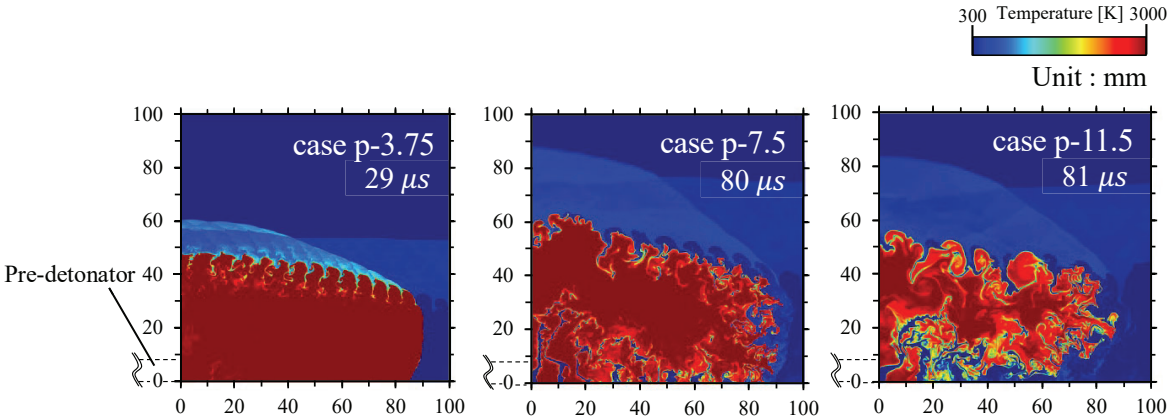

Figure 8. Instantaneous temperature fields of each premixed case

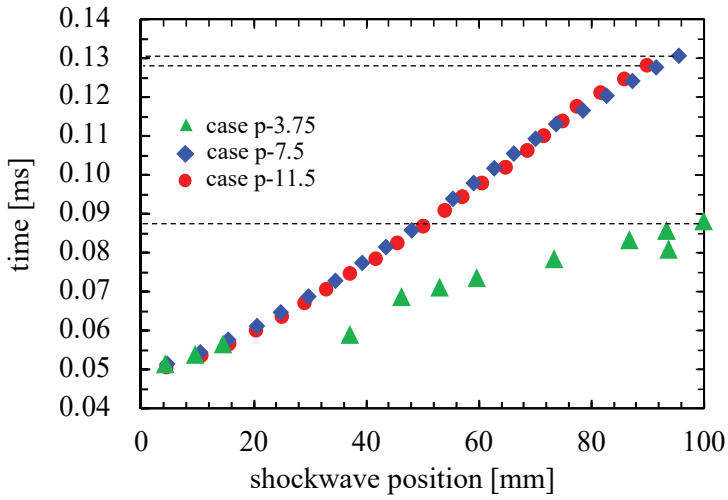

Figure 9. History of the position of shock wave at y=18 mm

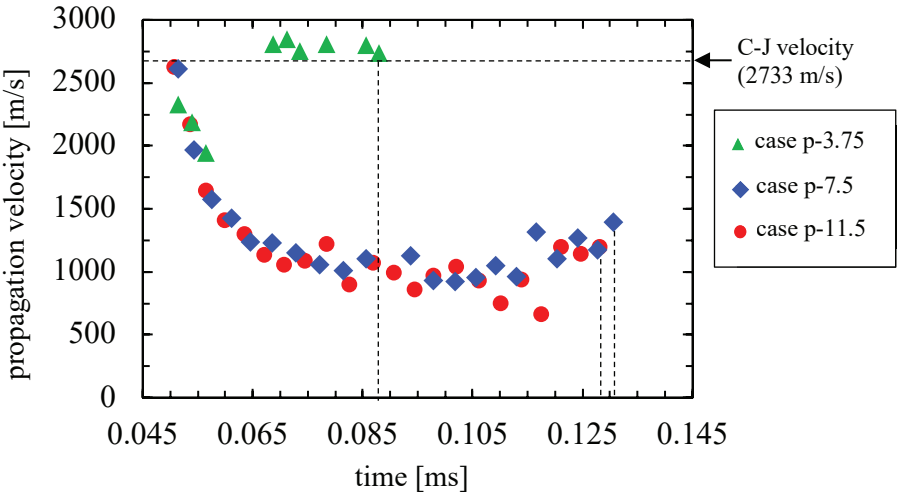

Figure 10. Time evolution of the propagation velocity at y=18 mm

Figure 11 shows the visualization of the area satisfying the flammable condition of hydrogen, and Fig. 12 shows its percentage of the total area of the leakage area. In the case of premixed inflow, the flammable area of hydrogen (volume fraction 4-94%) generally increases monotonically from the start with detonation entry, indicating an expansion of the flammable area.

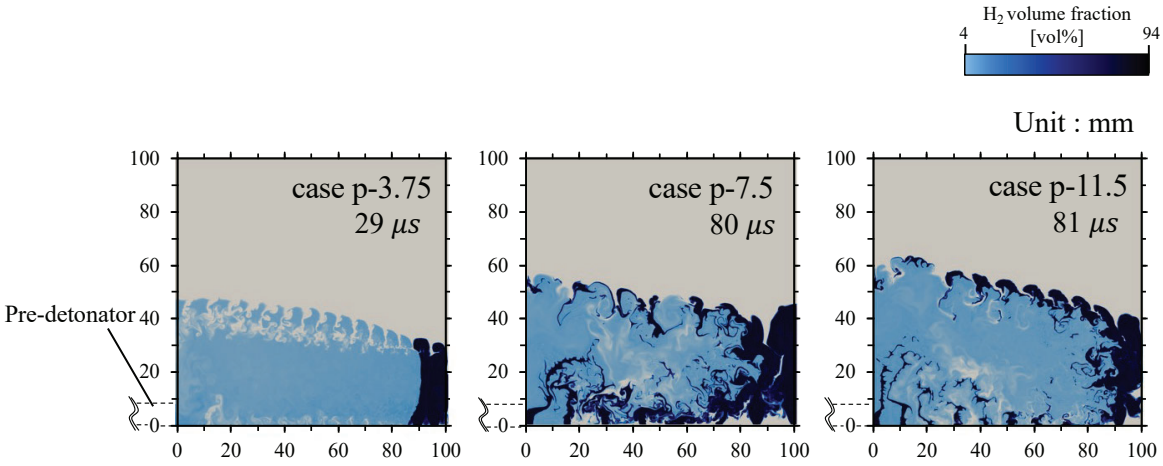

Figure 11. Visualization of the flammable area

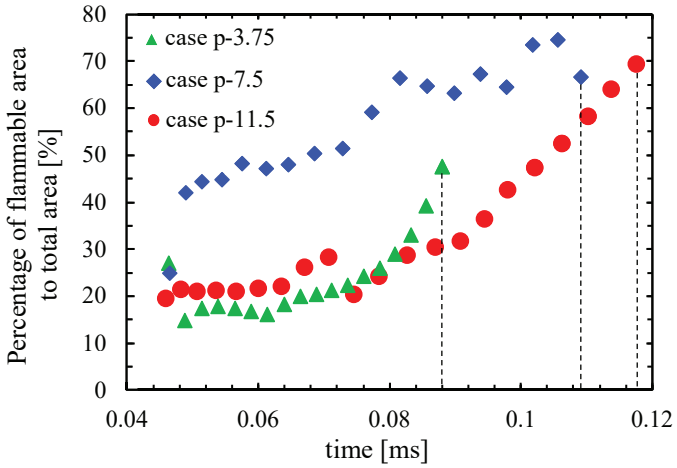

Figure 12. Time history of the percentage of flammable area

4.3 Behavior in non-premixed H_2-O_2 leakage

Figures 13 and 14 show instantaneous pressure and temperature fields, 92 μs, 96 μs , and 88 μs for each case after the detonation entered in leakage area under the non-premixed H_2-O_2 leaked condition. In Fig. 13 and 14, in all cases with non-premixed gas leakage from the bottom, the shock wave and the reaction zone were decoupled, and detonation did not maintain propagation under any of the conditions with different equivalent ratios. From these results, the detonation propagation was not maintained in the non-premixed inflow condition, even though the propagation was maintained in the premixed inflow condition.

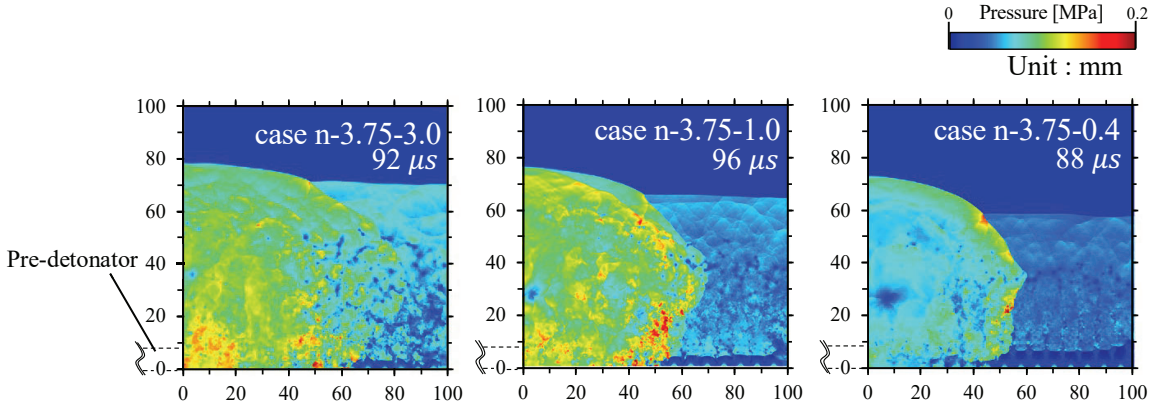

Figure 13. Instantaneous pressure fields of each non-premixed case

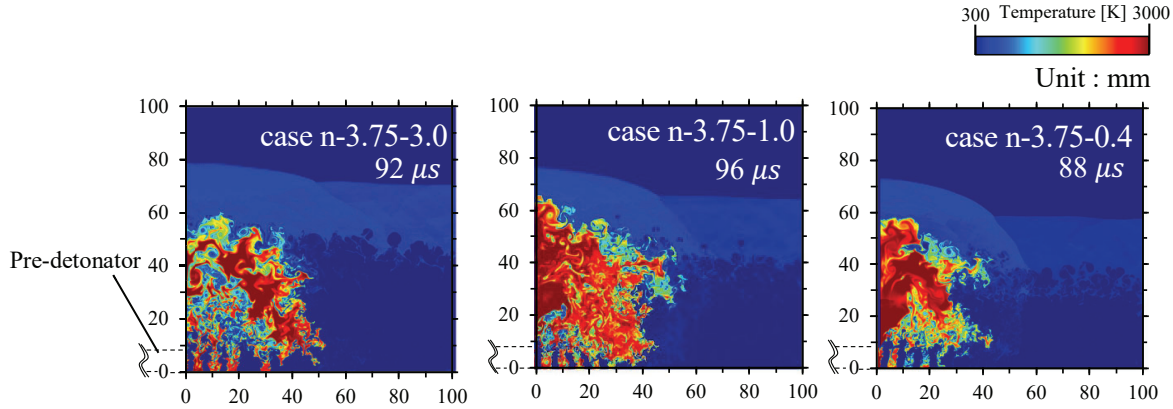

Figure 14. Instantaneous temperature fields of each non-premixed case

Figures 15 and 16 show the position of the leading shock wave and the reaction zone, as well as the time variation of the distance of these three cases. In Fig. 15 and 16, the distance between the leading shock wave and the reaction zone increased with time in all cases of non-premixed inflow. In addition, these distances increased slightly faster in the order of decreasing equivalence ratios.

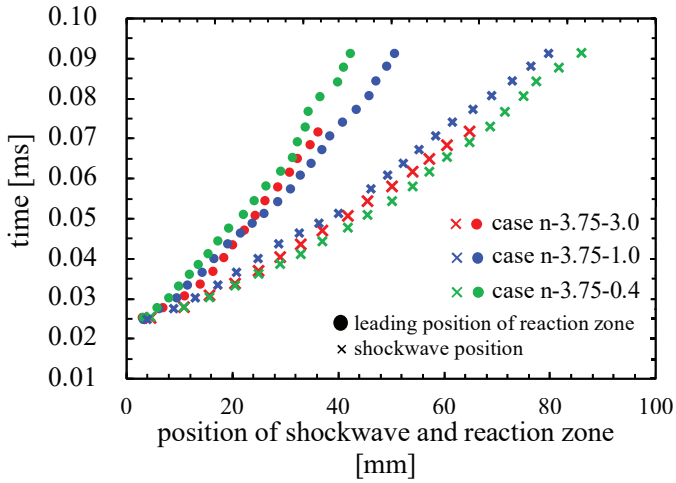

Figure 15. Time history of position of shock wave and reaction zone at y=18 mm

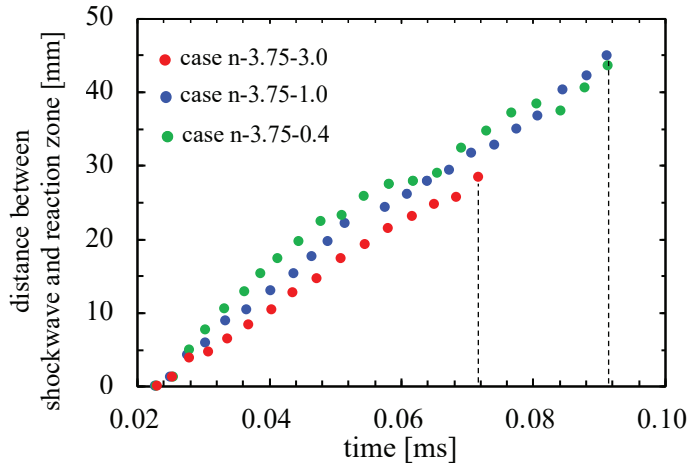

Figure 16. Time history of the distance between shockwave and reaction zone at y=18 mm

Figure 17 shows the visualization of the area satisfying the flammable condition of hydrogen, and Fig. 18 shows its percentage of the total area of the leakage area. In the case of the non-premixed inflow, the combustible zone was much narrower than in the case of the premixed inflow, and the change was only on the order of 0-6% after the start of detonation entry.

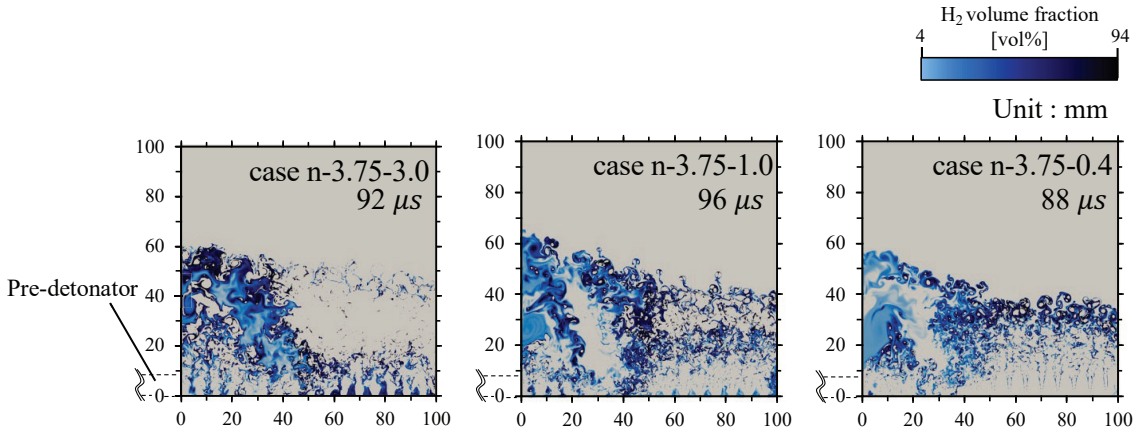

Figure 17. Visualization of the flammable area

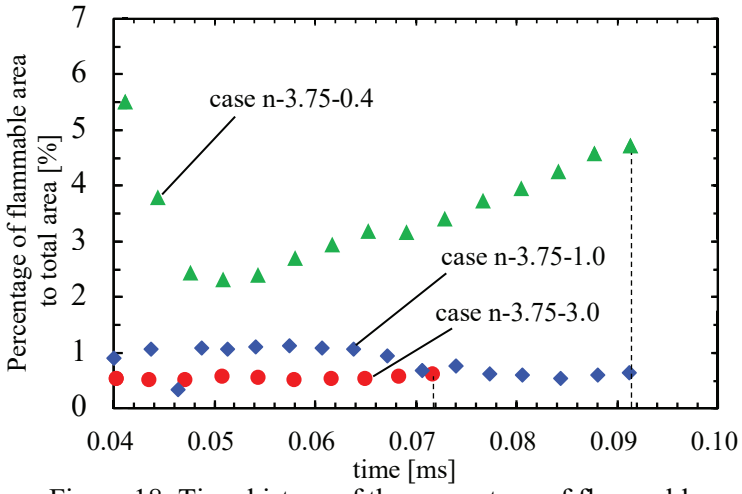

Figure 18. Time history of the percentage of flammable area

5.0 CONCLUSION

In this study, two-dimensional numerical analyses were conducted for the detonation propagating in combustible H_2-O_2 jet trains to clarify the combustion behavior where the hydrogen leaking area.

The following findings are obtained by analyzing three leakage conditions that were close to reality, starting from the most modeled leakage condition:

- Detonation entered in H_2-O_2 premixed gas uniformly distributed, and the shock wave gradually weakened as it propagated, suggesting that sufficient pressure build-up by combustion had not been achieved.

- Detonation entered in H_2-O_2 premixed gas leaking from the multiple leaking ports. Shock wave and reaction zone were coupled immediately behind, and detonation propagation sustainability can be observed. In particular, case p-3.75, with the most significant amount of leakage, had the strongest developed detonation compared to the other cases.

- Detonation entered during leakage of non-uniform H_2-O_2 non-premixed gas with different equivalent ratios. The detonation propagation was not maintained in the non-premixed inflow condition, even though the propagation was maintained in the premixed inflow condition.

ACKNOWLEDGMENTS

This study was financially supported by JSPS KAKENHI Grants No. JP19H05464, JP23H05446, by the Institute of Space and Astronautical Science of the Japan Aerospace Exploration Agency, and by Joint Usage/Research Center for Interdisciplinary Large-scale Information Infrastructures No. jh230050. Part of the numerical results in this research were obtained using supercomputing resources at Cyberscience Center, Tohoku University.

REFERENCES

1. International Civil Aviation Organization, Environmental Report, Montreal, pp. 1-248, 2016
2. Wierzba, I., and Kilchyk, V., Flamability limits of hydrogen-carbon monoxide mixtures at moderately elevated temperatures. International Journal of Hydrogen Energy, 26, pp.639-643, 2001
3. Zeldovich, Y.B, To the Question of Energy Use of Detonation Combustion, Journal of Propulsion and Power, 22, No. 3, 2006, pp. 588-592.
4. Burr, J.R., Yu, Ken, H., Experimental characterization of RDE combustor flow field using linear channel, Proceedings of the Combustion Institute, 37, No. 3, 2019, pp. 3471–3478.
5. Faming, W., Mizukaki, T., Matsuyama, S., Visualization and CFD of the influence of mixing on detonation wave propagation inside a rotating-detonation engine by using linear detonation channel, AIAA Scitech 2022 Forum, 3-7 January 2022, San Diego.
6. Wada, Y., Liou, M., An Accurate and Robust Flux Splitting Scheme for Shock and Contact Discontinuities, Journal of Scientific Computing, 18, 1997.
7. Gottlieb, S., Chi-wang, S., Total Variation Diminishing Runge-Kutta Schemes, Mathematics of Computation, 67, 1998.
8. Hong, Z., Davidson, D.F., Hanson, R.K., An improved H_2/O_2 mechanism based on recent shock tube/laser absorption measurements, Combustion and Flame, 158, 2011, pp. 633-644.